Mechanisms of Signal Transduction:

Cell Signaling Microdomain with Na,K-ATPase and Inositol 1,4,5-Trisphosphate Receptor Generates Calcium Oscillations

Ayako Miyakawa-Naito, Per Uhlén, Mark Lal, Oleg Aizman, Katsuhiko Mikoshiba, Hjalmar Brismar, Sergey Zelenin and Anita Aperia

J. Biol. Chem. 2003, 278:50355-50361.
doi: 10.1074/jbc.M305378200 originally published online August 28, 2003

THE JOURNAL OF BIOLOGICAL CHEMISTRY
Vol. 278, No. 50, Issue of December 12, pp. 50355–50361, 2003
Printed in U.S.A.

Cell Signaling Microdomain with Na,K-ATPase and Inositol 1,4,5-Trisphosphate Receptor Generates Calcium Oscillations*

Received for publication, May 22, 2003, and in revised form, August 20, 2003
Published, JBC Papers in Press, August 28, 2003, DOI 10.1074/jbc.M305378200

Ayako Miyakawa-Naito‡, Per Uhlén‡, Mark Lal, Oleg Aizman, Katsuhiko Mikoshiba§, Hjalmar Brismar, Sergey Zelenin, and Anita Aperia¶

From the Department of Woman and Child Health, Karolinska Institutet, Astrid Lindgren Children's Hospital, S-171 76 Stockholm, Sweden and the §Department of Basic Medical Science, The Institute of Medical Science, The University of Tokyo, 4-6-1 Shirokanedai, Minato-ku, Tokyo 108-8639, Japan

Recent studies indicate novel roles for the ubiquitous ion pump, Na,K-ATPase, in addition to its function as a key regulator of intracellular sodium and potassium concentration. We have previously demonstrated that ouabain, the endogenous ligand of Na,K-ATPase, can trigger intracellular Ca^{2+} oscillations, a versatile intracellular signal controlling a diverse range of cellular processes. Here we report that Na,K-ATPase and inositol 1,4,5-trisphosphate ($InsP_3$) receptor ($InsP_3R$) form a cell signaling microdomain that, in the presence of ouabain, generates slow Ca^{2+} oscillations in renal cells. Using fluorescent resonance energy transfer (FRET) measurements, we detected a close spatial proximity between Na,K-ATPase and $InsP_3R$. Ouabain significantly enhanced FRET between Na,K-ATPase and $InsP_3R$. The FRET effect and ouabain-induced Ca^{2+} oscillations were not observed following disruption of the actin cytoskeleton. Partial truncation of the NH_2 terminus of Na,K-ATPase catalytic α1-subunit abolished Ca^{2+} oscillations and downstream activation of NF-κB. Ouabain-induced Ca^{2+} oscillations occurred in cells expressing an $InsP_3$ sponge and were hence independent of $InsP_3$ generation. Thus, we present a novel principle for a cell signaling microdomain where an ion pump serves as a receptor.

Na,K-ATPase is an integral membrane protein expressed in all eukaryotic cells, where it functions as a key regulator of intracellular Na^+ and K^+ concentrations (1). Recent studies, however, point to an additional role for Na,K-ATPase as a signal transducer (2–5). Importantly, Na,K-ATPase has an endogenous ligand, ouabain, a steroid hormone that dose-dependently inhibits the activity of Na,K-ATPase. The biological role of ouabain is, despite extensive research, not well understood. Ouabain belongs to the family of cardiac glycosides, which have been used for centuries in the treatment of heart disease. Recently, several investigators have noted that cardiac glycosides may act as anticancer agents (6, 7).

We have described a new cell signaling pathway triggered by ouabain (2). Using rat renal proximal tubule (RPT)[1] cells, we showed that exposure to concentrations of ouabain that cause only partial inhibition of Na,K-ATPase activity induces slow intracellular Ca^{2+} oscillations and subsequent activation of the transcription factors NF-κB and cAMP-response element-binding protein. Our results from that study indicated that Ca^{2+} oscillations occurred as an interplay between different Ca^{2+} transporters and that Ca^{2+} release via the inositol 1,4,5-trisphosphate ($InsP_3$) receptor ($InsP_3R$) was involved in this event. Na,K-ATPase does not possess the characteristics of a G-protein-coupled receptor. Given the generality of Na,K-ATPase expression and its significant role in cell homeostasis, it is important to identify the molecular mechanisms by which Na,K-ATPase can act as a signal transducer. Here we show that the generation of Ca^{2+} oscillations by ouabain is dependent on the physical association of Na,K-ATPase and $InsP_3R$ in a signaling microdomain.

EXPERIMENTAL PROCEDURES

Expression Plasmids—A cDNA fragment encoding wild type rat Na,K-ATPase α1-subunit (NKAα1) was amplified by AmpliTaq Gold (Applied Biosystems). The PCR product was digested by ApaI/XbaI restriction enzymes and cloned into pEGFP-C2 (Clontech) to obtain pGFP-NKAα1. A mutant NKAα1 with truncation of the first 32 amino acids (NKAα1.M32) was generated using PCR. The region of truncation of the NH_2 terminus was decided on the basis of structure/function analysis reported elsewhere (8). The sense primer sequence was 5′-AAAGGGCCCATGGAAGTGTCTATGGACGAC-3′, corresponding to nucleotide positions 349–366 of NKAα1 (GenBank™ accession number NM_012504) with an additional ApaI site and ATG codon on the 5′-end of the primer. The antisense primer was 5′-CTTGCCGTGGAGGAGGATAGAACT-3′, corresponding to nucleotide positions 1792–1815 of NKAα1. The PCR product and pGFP-NKAα1 were hydrolyzed by ApaI/AflII restriction enzymes and ligated for cloning pGFP-NKAα1.M32.

A fusion protein with NH_2-terminal glutathione *S*-transferase (GST) and 95 amino acids of NKAα1 (GST-NKAα1.N95) was constructed using Gateway Technology (Invitrogen). Briefly, a cDNA fragment encoding 95 amino acids of the Na,K-ATPase α1-subunit NH_2 terminus was amplified by AmpliTaq Gold (Applied Biosystems). The PCR product was cloned in pENTR/D-TOPO vector using pENTR Directional TOPO cloning kit (Invitrogen) and subcloned into pDEST-15 using Gateway System (Invitrogen) to obtain pGST-NKAα1.N95. The nucleotide sequences of all constructs were confirmed by automated sequencing (KISEQ, Core Facilities of Karolinska Institutet, Stockholm, Sweden) and subsequent bioinformatics analysis using Lasergene software (DNASTAR).

* This work was supported by grants from the Swedish Research Council, the Persson Family Foundation, the Märta and Gunnar V. Philipson Foundation (to A. A. and H. B.), Japan Science and Technology Corporation "Calcium Oscillation Project" (to K. M. and A. A.), and the Ministry of Education, Science, Sports and Culture of Japan (to A. M.-N.). The costs of publication of this article were defrayed in part by the payment of page charges. This article must therefore be hereby marked "*advertisement*" in accordance with 18 U.S.C. Section 1734 solely to indicate this fact.

‡ Both authors contributed equally to this work.

¶ To whom correspondence should be addressed: Dept. of Woman and Child Health, Karolinska Institutet, Astrid Lindgren Children's Hospital, Q2:09, S-171 76 Stockholm, Sweden. Tel.: 46-8-51777326; Fax: 46-8-51777328; E-mail: anita.aperia@ks.se.

[1] The abbreviations used are: RPT, renal proximal tubule; $InsP_3$, inositol 1,4,5-trisphosphate; $InsP_3R$, inositol 1,4,5-trisphosphate receptor; FRET, fluorescent resonance energy transfer; PLC, phospholipase C; ER, endoplasmic reticulum; SERCA, sarco-endoplasmic reticulum Ca^{2+} ATPase; CPA, cyclopiazonic acid; 2-APB, 2-aminoethoxydiphenyl borate; CytD, cytochalasin D; AQP4, aquaporin-4; GST, glutathione *S*-transferase; GFP, green fluorescent protein; EGFP, enhanced GFP.

For FRET control experiments, the cytosolic NH_2 terminus of aquaporin-4 (AQP4) was tagged with GFP to obtain pGFP-AQP4 (9). InsP$_3$R type 1 ligand binding protein (226–604 amino acids) with point mutation (R441Q) encoding InsP$_3$ sponge was cloned into a pEF-BOS-MCS vector (pEF-GSTm49-IRES-GFP) (10). pEGFP-actin was from Clontech.

Cell Culture and Transfections—Three types of renal cells were used: primary cultures of rat RPT cells prepared as described (11), COS-7 cells, a cell line derived from fetal monkey kidney, and LLC-PK$_1$ cells, a cell line derived from pig kidney. GFP-NKAα1 was stably expressed in COS-7 cells (12). pGFP-NKAα1, pGFP-NKAα1.M32, pEF-GSTm49-IRES-GFP, or pEGFP-actin was transiently transfected into RPT cells on culture day 2 using CLONfectin (Clontech). pGFP-AQP4 was transiently transfected into COS-7 cells on culture day 2 using CLONfectin (Clontech).

Reagents—Reagents were used at the following concentrations: 20 μM cyclopiazonic acid (CPA), 5 μM cytochalasin D (CytD), 100 pM-250 μM ouabain, 5 μM 2-aminoethoxydiphenyl borate (2-APB), 0.5 μM bradykinin, and 5 μM U73122. All reagents were from Sigma.

Intracellular Calcium and Sodium Measurements—Intracellular Ca^{2+} and Na^+ measurements were performed using Fura-2/AM and SBFI/AM (Molecular Probes), respectively, as described previously (2, 11). After baseline recording, cells were treated, and ratio images were recorded every 30 s for 45–90 min. In each dish, 20–30 individual cells from a single cluster of cells were analyzed. Results presented are representative single cell traces obtained from a minimum of 12 experiments.

Immunocytochemistry and Confocal Microscopy—For co-immunolocalization and FRET studies, COS-7 cells stably expressing GFP-NKAα1 were fixed with acetone for 3 min at room temperature and then incubated with phosphate-buffered saline containing 5% (v/v) normal goat serum and 3% (w/v) bovine serum albumin for 1 h. InsP$_3$Rs were probed with monoclonal mouse anti-rat InsP$_3$R type 2 (KM1083) or type 3 (KM1082) antibodies (1 μg/ml) (13) overnight at 4 °C. Cy3-conjugated goat anti-mouse IgG antibody served as secondary antibody (1:1000, Jackson ImmunoResearch Laboratories). Cells were scanned with a Leica TCS SP inverted confocal scanning laser microscope.

NF-κB activation was measured in RPT cells by immunocytochemical staining as described previously (2). RPT cells transiently transfected with pGFP-NKAα1.M32 were treated with 250 μM ouabain for 30 min and then fixed using 3% paraformaldehyde (10 min). Following blocking as described above, cells were incubated with NF-κB p65 antibody (1:200, Santa Cruz Biotechnology) for 1 h and then with Alexa 546 fluorescent secondary antibody (1:500, Molecular Probes) for 30 min. Slides were scanned using a Leica TCS SP inverted confocal scanning laser microscope, and images of cells expressing the construct were identified by GFP signal; NF-κB immunostaining of cells was captured for the same field of view. NF-κB activation in individual cells was semiquantitatively estimated by measuring the ratio between the mean NF-κB immunosignal in a given comparable area in the nucleus and cytoplasm in cells expressing GFP-NKAα1.M32 or those adjacent cells not expressing the construct using ImageJ (Wayne Rasband, National Institutes of Health).

FRET—Fluorescent resonance energy transfer (FRET) measurements were performed on a Leica TCS SP inverted confocal scanning laser microscope using a ×40/1.4 NA objective. A detailed description of the FRET technique can be found elsewhere (14, 15). The Förster constant, R_0, for the donor-acceptor pair, GFP and Cy3, used in this study was 6 nm (16). FRET occurs when the fluorophores are separated by distances $0.5\ R_0 < r < 2\ R_0$. Thus, it is possible to distinguish proteins that are spatially co-localized within a 12-nm radius. To determine FRET, we quantified the quenching of donor fluorescence by performing acceptor photobleaching (14). COS-7 cells stably expressing GFP-NKAα1 and stained with Cy3-labeled secondary goat anti-mouse IgG secondary antibody (Jackson ImmunoResearch Laboratories) to detect mouse monoclonal antibody to InsP$_3$R2 (KM1083) and InsP$_3$R3 (KM1082) were excited with 488 and 543 nm and collected separately. The acceptor, Cy3, was then irreversibly photobleached in a selected adequate region by continuous excitation with 543 and 633 nm lasers for 30–90 s. Thereafter, the residual Cy3 and GFP image was obtained, and identical regions, at the plasma membrane on individual cells, were outlined in the photobleached area and processed using ImageJ (Wayne Rasband, National Institutes of Health). Ratios between GFP intensities of the plasma membrane region, after and before photobleaching, were calculated to quantify FRET. The FRET values presented are corrected for erroneous intensity changes in a selected region outside the bleached area. In a typical experiment, 10–15 cells were measured for each sample.

Immunoprecipitation Studies—Cells were solubilized in lysis buffer (50 mM Tris/HCL (pH 7.4), 150 mM NaCl, 0.25% sodium deoxycholate, 1% Triton X-100, 1 mM phenylmethylsulfonyl fluoride, protease inhibitors (Roche Applied Science)) and left for 30 min on ice. Cell lysates were sonicated (3 × 2 s at setting 2 using a Branson Sonifier 250, Branson Ultrasonics) and centrifuged at 9,000 × *g* at 4 °C to obtain a crude cell extract. 500 μg of supernatant protein/reaction were precleared with protein G-Sepharose for 1 h to reduce background that may be caused by non-specific adsorption of cellular debris. After a low speed centrifugation, the resultant supernatant was incubated for 1 h at 4 °C with a mouse monoclonal anti-Na,K-ATPase α1-subunit antibody (1:250; Upstate Biotechnology), a mouse monoclonal anti-InsP$_3$R2 antibody (1:50; Santa Cruz Biotechnology), or a mouse monoclonal antibody anti-InsP$_3$R3 antibody (1:50; BD Biosciences). Immunocomplexes were incubated with protein G-Sepharose beads overnight at 4 °C. Beads were pelleted, washed, and incubated with 2× Laemmli buffer, and supernatants were subjected to SDS gel electrophoresis using 6% acrylamide gels. Membranes were incubated overnight with a mouse monoclonal anti-InsP$_3$R3 antibody (1 μg/ml; KM1082) and then for 1 h using a horseradish peroxidase-conjugated secondary antibody (1:5000) prior to detection using ECL plus (Amersham Biosciences). The resultant protein bands were scanned digitally and densitometrically analyzed by Bio-Rad QuantitativeOne software.

GST Pull-down Assay—GST-NKAα1.N95 was produced in the BL21 strain of *Escherichia coli* and purified with glutathione-Sepharose 4B beads (Amersham Biosciences). Non-recombinant GST was used as a control. Detergent-extracted RPT cell lysate (prepared as described above for the co-immunoprecipitation protocol) was added to the beads in a 5:1 ratio (v/v) and incubated overnight at 4 °C with gentle rotation. Beads were washed and resuspended in 2× Laemmli buffer prior to SDS gel electrophoresis (6% gel) and immunoblotting for InsP$_3$R3.

Data Presentation and Analysis—Data are presented as means ± S.E. of a minimum of 10 experiments, unless indicated otherwise. Student's *t* test was used, and significance was accepted at $p < 0.05$.

RESULTS

In accordance with previous observations (2), ouabain (250 μM) induced highly regular intracellular Ca^{2+} oscillations with a periodicity in the minute range in RPT cells (Fig. 1*a*). Typical Ca^{2+} oscillations were detected about 5–15 min after ouabain exposure in approximately one-third of the cells and were generally initiated in one cell at the periphery of a cell cluster. Quantitatively and qualitatively, COS-7 cells treated with ouabain showed a similar Ca^{2+} oscillatory response (Fig. 1*b*). Spontaneous oscillations in cytosolic Ca^{2+} were never observed in untreated cells. Na,K-ATPase activity is dose-dependently inhibited by ouabain, and 250 μM ouabain causes ~50% inhibition of rat Na,K-ATPase activity (2). Ouabain, 250 μM, exceeds circulating levels in rat, estimated to be in the pM-nM range (17). When cells were exposed to physiological ouabain doses (100 pM), Ca^{2+} oscillations were observed (Fig. 1*c*) in ~1% of cells. For subsequent experiments designed to explore the mechanism by which Na,K-ATPase triggers Ca^{2+} oscillations, we used 250 μM ouabain.

To elucidate the source of the Ca^{2+} oscillatory response, intracellular endoplasmic reticulum (ER) Ca^{2+} stores were depleted by preincubation with a sarco-endoplasmic reticulum Ca^{2+} ATPase (SERCA) inhibitor, CPA (Fig. 1*d*). Ouabain did not induce Ca^{2+} oscillations in CPA-pretreated cells. Regulated Ca^{2+} release from intracellular ER Ca^{2+} stores occurs mainly via InsP$_3$Rs or via ryanodine receptors. InsP$_3$Rs are abundantly expressed in RPT cells, whereas ryanodine receptors do not have any functional importance for ouabain-triggered Ca^{2+} oscillations in these cells (2). The membrane-permeable substance, 2-APB, was initially introduced as a specific inhibitor of InsP$_3$Rs (18). The IC_{50} for inhibition of InsP$_3$R-evoked Ca^{2+} release was reported to be 1–20 μM. Since then, 2-APB has, in addition to its inhibitory effect on InsP$_3$-induced Ca^{2+} release, been shown to block store-operated calcium-mediated cytosolic Ca^{2+} influx (19). Store-operated calcium is generally fully inhibited by 50–100 μM 2-APB. Exposure of cells to concentrations of 2-APB higher than 100 μM may also cause a pro-

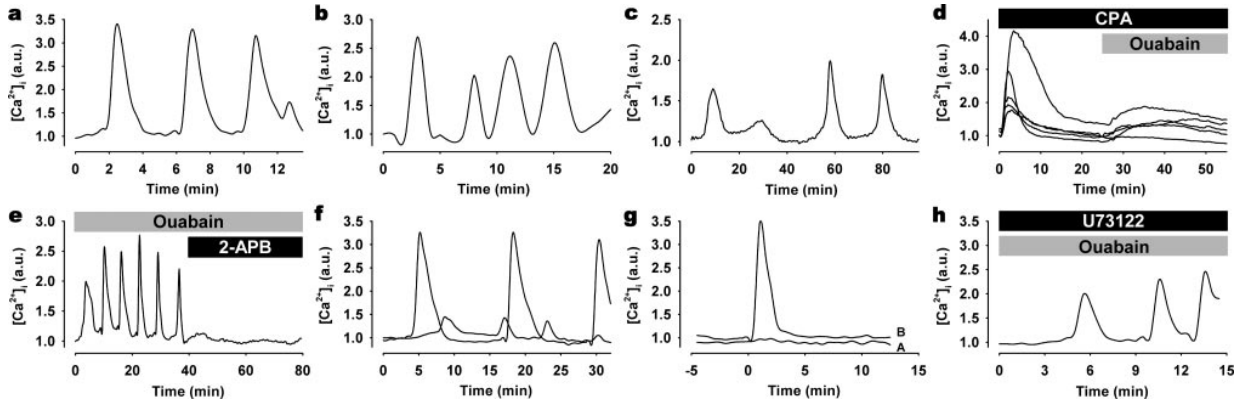

FIG. 1. **Intracellular Ca^{2+} response to ouabain in renal cells.** *a–c*, Ca^{2+} oscillations in 250 μM ouabain-treated RPT cells (*a*), 250 nM ouabain-treated COS-7 cells (*b*), and 100 pM ouabain-treated RPT cells (*c*). Arbitrary units (*a.u.*) represent ratio values corresponding to intracellular Ca^{2+} concentration changes. In *d*, CPA depleted intracellular ER Ca^{2+} stores and abolished ouabain-induced Ca^{2+} oscillations in RPT cells. Each trace represents a single cell recording. In *e*, ouabain-induced Ca^{2+} oscillations in RPT cells were abolished by 2-APB (5 μM). *f*, two representative single cell recordings of cytosolic Ca^{2+} in RPT cells transfected with the $InsP_3$ sponge (n = 15). The amplitude was lower in some $InsP_3$ sponge-expressing cells. *g*, two representative single cell recordings of cytosolic Ca^{2+} in RPT cells. Bradykinin did not induce Ca^{2+} transients in $InsP_3$ sponge-expressing RPT cells (*trace A*), whereas non-transfected cells exhibited Ca^{2+} transients (*trace B*). In *h*, U73122 (5 μM) did not abolish ouabain-induced Ca^{2+} oscillations in RPT cells.

nounced increase of basal cytosolic Ca^{2+}, consistent with inhibition of the SERCA pump (19). Since available data suggest that low concentrations (up to 20 μM) of 2-APB will preferentially inhibit $InsP_3$Rs, we tested the effect of 5 μM 2-APB. Using this concentration, we found that ouabain-induced Ca^{2+} oscillations were abolished in the majority of cells treated with 2-APB (5 μM) (Fig. 1*e*). Collectively, the inhibitory effects of CPA and 2-APB demonstrate that release of Ca^{2+} via $InsP_3$R is an essential contributor to the Ca^{2+} oscillations triggered by the ouabain/Na,K-ATPase complex.

Activation of $InsP_3$Rs is critically dependent on activation of phospholipase C (PLC), phosphatidylinositol lipid hydrolysis, and liberation of $InsP_3$. Notably, however, recent studies indicate that $InsP_3$R function is also modulated by interaction with accessory proteins (20–22). To examine the role of $InsP_3$ for the ouabain-induced Ca^{2+} oscillations, RPT cells were transfected with a construct encoding a hyper-affinity $InsP_3$ absorbent, an $InsP_3$ sponge. The $InsP_3$ sponge, having more than 1000-fold higher affinity for $InsP_3$ than $InsP_3$R, traps $InsP_3$ and abrogates $InsP_3$-induced Ca^{2+} release (10). The construct also encoded GFP to facilitate identification of transfected cells. Ouabain triggered low frequency Ca^{2+} oscillations in one-third of the cells expressing the $InsP_3$ sponge (Fig. 1*f*). The amplitude of the oscillatory response was attenuated in some, but not all, of the cells expressing the $InsP_3$ sponge. To confirm the efficiency of the $InsP_3$ sponge in quenching $InsP_3$-mediated Ca^{2+} signaling in RPT cells, we treated cells with bradykinin, a well known activator of PLC and $InsP_3$ production (23). Bradykinin induced single Ca^{2+} transients in virtually all non-transfected cells but was without effect in all cells expressing the $InsP_3$ sponge (Fig. 1*g*). Cells expressing only GFP exhibited regular ouabain-induced Ca^{2+} oscillations (data not shown). It was further found that preincubation of RPT cells with a PLC inhibitor, U73122, abolished bradykinin-induced Ca^{2+} transients (data not shown) but did not influence ouabain-induced Ca^{2+} oscillations (Fig. 1*h*). These findings indicate that ouabain-induced Ca^{2+} oscillations do not require increased $InsP_3$ levels to activate $InsP_3$R in this model.

Immunocytochemical studies, performed on COS-7 cells, revealed partial co-localization of Na,K-ATPase with $InsP_3$R types 1, 2, and 3 ($InsP_3$R1, $InsP_3$R2, and $InsP_3$R3), respectively. Only $InsP_3$R2 (Fig. 2*a*) and $InsP_3$R3 (Fig. 2*b*) were studied in subsequent experiments since these isoforms were more abundantly expressed than $InsP_3$R1. To investigate the

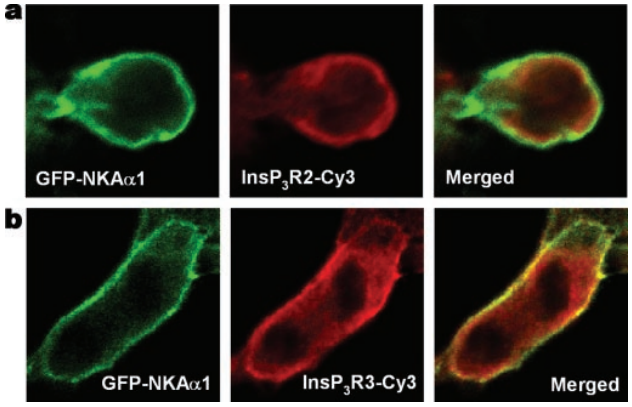

FIG. 2. **Immunocytochemical studies of Na,K-ATPase and $InsP_3$R localization in COS-7 cells.** Na,K-ATPase (GFP-NKAα1) and $InsP_3$R2 ($InsP_3$R2-Cy3) (*a*) or $InsP_3$R3 ($InsP_3$R3-Cy3) (*b*) co-localize near the plasma membrane.

spatial relationship between Na,K-ATPase and $InsP_3$R on a nanometer scale, FRET measurements were performed. In this protocol, we used COS-7 cells stably expressing GFP-tagged Na,K-ATPase α1-subunit. These cells express approximately the same level of Na,K-ATPase as wild type COS-7 cells (12). GFP, which was fused to the cytosolic NH_2 terminus of Na,K-ATPase, served as FRET donor (GFP-NKAα1). The primary antibodies against $InsP_3$R2 or $InsP_3$R3 were probed with a Cy3-conjugated IgG secondary antibody, which served as the FRET acceptor ($InsP_3$R-Cy3). The epitopes recognized by the $InsP_3$R2 and $InsP_3$R3 antibodies are located in the cytoplasmic COOH terminus of the respective $InsP_3$Rs (13). The GFP-NKAα1 fluorescence intensity was, following acceptor photobleaching, enhanced 12.5 ± 0.9% for $InsP_3$R2 and 15.5 ± 2.0% for $InsP_3$R3 (Fig. 3, *a* and *b*). These results imply that the donor and acceptor complexes, GFP-NKAα1 and anti-$InsP_3$R-anti-mouse IgG-Cy3, were separated less than 12 nm, *i.e.* the maximal distance for FRET detection between GFP and Cy3 (16). Ouabain treatment significantly increased FRET (from 15.5 ± 2.0% to 25.0 ± 1.6%) between Na,K-ATPase and $InsP_3$R (Fig. 3, *a* and *b*).

To confirm that the observed FRET between Na,K-ATPase and $InsP_3$R3 was a unique property of this pair of proteins and not merely the result of non-specific experimental artifacts, we

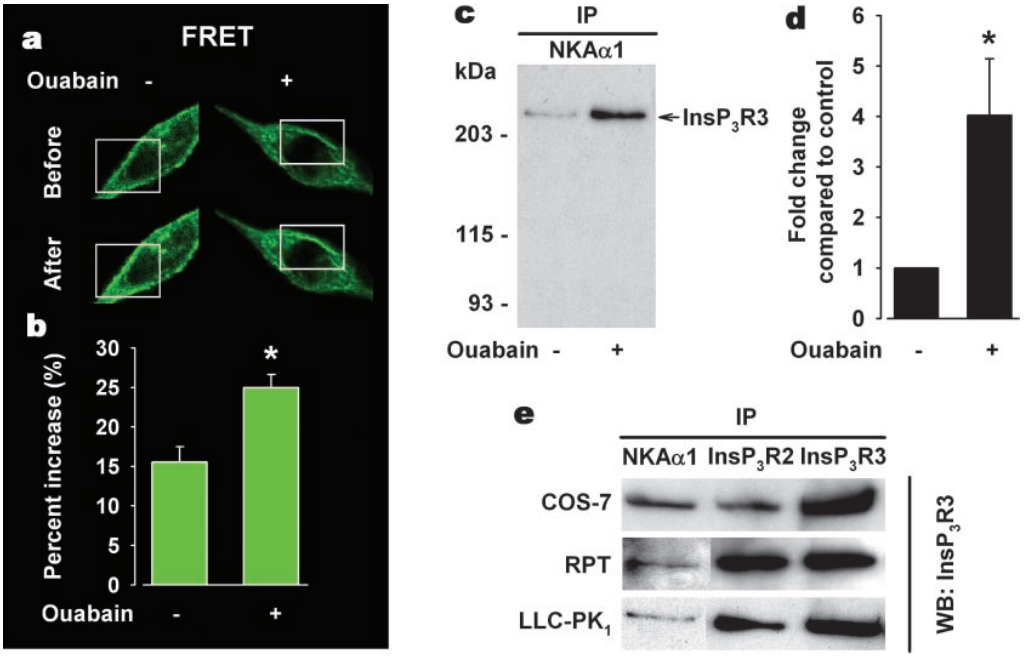

FIG. 3. **Studies of Na,K-ATPase and InsP$_3$R signaling microdomain.** *a* and *b*, FRET measurements between Na,K-ATPase and InsP$_3$R3. *a*, GFP-NKAα1 images of COS-7 cells with and without ouabain treatment before and after acceptor photobleaching (bleached area indicated by *square*). *b*, quantitative changes in emission intensities after bleaching as compared with before bleaching, mean ± S.E., *, $p < 0.05$. FRET was enhanced by ouabain. *c–e*, co-immunoprecipitation (*IP*) studies followed by Western blotting (*WB*) for InsP$_3$R3. *c* and *d*, representative Western blot (*c*) and densitometric analysis (*d*) of InsP$_3$R3 content in Na,K-ATPase immunoprecipitates before and after 250 μM ouabain treatment for 30 min in COS-7 cells. Ouabain significantly increased the amount of InsP$_3$R3 associated with Na,K-ATPase, mean ± S.E. ($n = 3$), *, $p < 0.05$. Molecular mass markers are indicated to the *left* of the blot. In *e*, InsP$_3$R3 co-immunoprecipitated with Na,K-ATPase and InsP$_3$R2 in COS-7, RPT and LLC-PK$_1$ cells.

designed control experiments using another integral plasma membrane protein, namely AQP4. For these negative control experiments, GFP-AQP4 was expressed in COS-7 cells. FRET analysis was performed using GFP-AQP4 (donor) and the same Cy3-labeled secondary antibody to detect the InsP$_3$R3 antibody (InsP$_3$R3-Cy3, acceptor). No change in donor emission ratio before and after acceptor photobleaching was found for this molecular pair (data not shown). This result indicates that FRET between Na,K-ATPase and InsP$_3$R3 is not likely a result of non-specific effects of the fixation protocol on plasma membrane and ER membrane integrity and strengthens the conclusion that the physical association between Na,K-ATPase and InsP$_3$R3 is specific.

Co-immunoprecipitation studies added further support to the concept that Na,K-ATPase and InsP$_3$R are linked together in a microdomain. As shown in Fig. 3*c*, InsP$_3$R3 co-immunoprecipitated with Na,K-ATPase in COS-7 cells. The amount of InsP$_3$R3 that co-immunoprecipitated with Na,K-ATPase represented only a fraction (<50%) of the total InsP$_3$R3 present in the initial cell lysate. Non-immune IgG did not co-immunoprecipitate a detectable amount of InsP$_3$R3 (data not shown). Incubation of COS-7 cells with ouabain significantly increased the amount of InsP$_3$R3 associated with immunoprecipitated Na,K-ATPase (Fig. 3, *c* and *d*). The propensity of InsP$_3$R3 to co-immunoprecipitate with Na,K-ATPase was also demonstrated in RPT and LLC-PK$_1$ cells (Fig. 3*e*). InsP$_3$R isoforms form heterotetrametric channels (24), and as expected, InsP$_3$R2 co-immunoprecipitated with InsP$_3$R3 in all cell types (Fig. 3*e*).

Both Na,K-ATPase and InsP$_3$R bind to cytoskeleton proteins that are anchored by the actin network (25, 26). To examine whether the signaling function of the Na,K-ATPase/InsP$_3$R complex depends on an intact cytoskeleton, RPT cells were pretreated with CytD to depolymerize the actin cytoskeleton (Fig. 4*a*). Ouabain-induced Ca^{2+} oscillations (Fig. 4*b*) and FRET between Na,K-ATPase and InsP$_3$R3 (Fig. 4, *c* and *d*) were completely abolished in CytD-pretreated cells. Also, no InsP$_3$R3 co-immunoprecipitated with Na,K-ATPase in cells pretreated with CytD (Fig. 4*e*). Bradykinin induced normal single Ca^{2+} transients in cells pretreated with CytD (data not shown).

The NH_2 terminus of Na,K-ATPase α1-subunit is a flexible part of the molecule (27, 28). We therefore initiated a series of experiments to test the cellular consequences of Na,K-ATPase NH_2-terminal truncation. RPT cells were transfected with a Na,K-ATPase α1-subunit mutant, where 32 amino acids from the NH_2 terminus were deleted (NKAα1.M32) (Fig. 5*a*). To identify transfected cells, NKAα1.M32 was tagged with GFP (GFP-NKAα1.M32). GFP-NKAα1.M32 was localized predominantly at the plasma membrane (Fig. 5*b*). This limited truncation was chosen because it does not significantly impact Na,K-ATPase function; truncation of 32 amino acids from the NH_2 terminus results in a functional enzyme that possesses similar Na^+/K^+ exchange properties when transfected into cells (29). To confirm the function of the truncated enzyme on single cells, the effect of ouabain on intracellular Na^+ concentration was monitored. Ouabain caused a similar increase in Na^+ in cells expressing GFP-NKAα1.M32 and cells that only expressed endogenous Na,K-ATPase (Fig. 5*c*), indicating not only that the mutant was a fully functioning enzyme but that it also preserved its capacity to bind ouabain. Ouabain-induced Ca^{2+} oscillations were not observed in GFP-NKAα1.M32-expressing cells (Fig. 5*d*), whereas cells expressing only endogenous Na,K-ATPase α1-subunit did oscillate. Cells transiently transfected with a GFP-tagged full-length Na,K-ATPase α1-subunit exhibited ouabain-triggered Ca^{2+} oscillations to the same extent as non-transfected cells (data not shown). These results indicate that the NH_2 terminus of Na,K-ATPase α1-subunit plays a

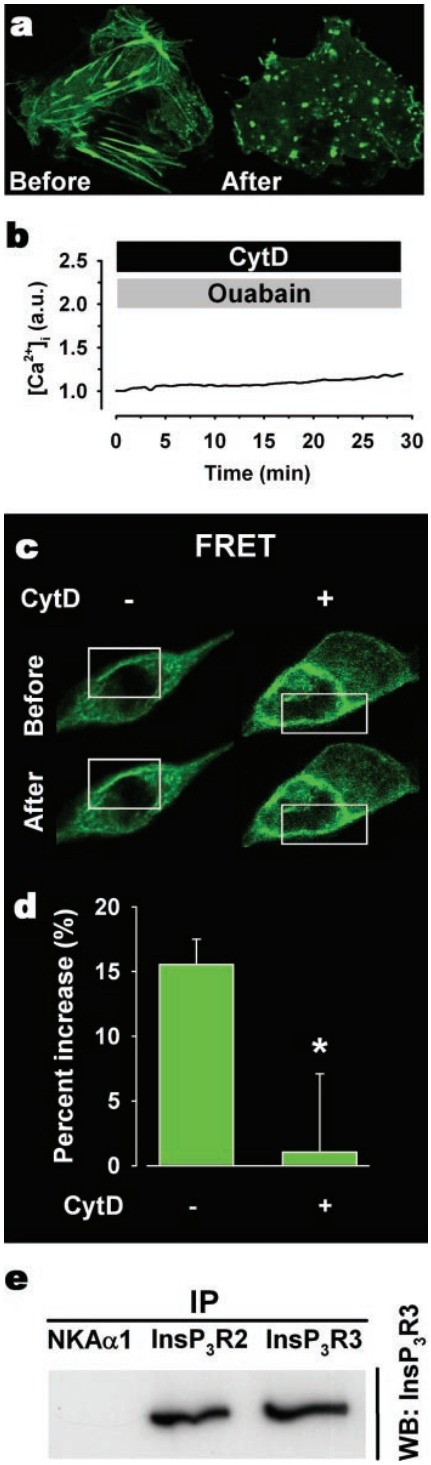

FIG. 4. **Effect of cytoskeleton perturbation on physical association between Na,K-ATPase and InsP$_3$R.** In *a*, the actin cytoskeleton was disrupted after CytD (5 μM) treatment in GFP-actin-expressing RPT cells. In *b*, CytD abolished ouabain-induced Ca^{2+} oscillations in RPT cells. Arbitrary units (*a.u.*) represent ratio values corresponding to intracellular Ca^{2+} concentration changes. *c* and *d*, FRET measurements between Na,K-ATPase and InsP$_3$R3. *c*, GFP-NKAα1 images of COS-7 cells with and without CytD treatment before and after acceptor photobleaching (bleached area indicated by *square*). *d*, quantitative changes in emission intensities after bleaching as compared with before bleaching, mean ± S.E., *, $p < 0.05$. FRET was eliminated by CytD. *e*, co-immunoprecipitation (*IP*) studies followed by Western blotting (*WB*) for InsP$_3$R3 in CytD-treated COS-7 cells. InsP$_3$R3 did not co-immunoprecipitate with Na,K-ATPase.

central role for induction of ouabain-induced Ca^{2+} oscillations. We also performed a GST pull-down assay where GST was fused to the full-length (95 amino acids) NH_2 terminus of the Na,K-ATPase α1-subunit. GST-NKAα1.N95 pulled down InsP$_3$R3 from a lysate of RPT cells, whereas GST alone did not pull down InsP$_3$R3 (Fig. 5*e*).

It was demonstrated previously that NF-κB, a well known Ca^{2+}-dependent transcription factor, is more readily activated by low frequency Ca^{2+} oscillations than by a sustained Ca^{2+} increase (30). To exploit this effect and to determine the downstream functional implications of disturbing the communication between the NH_2 terminus of Na,K-ATPase α1-subunit and InsP$_3$R, we compared NF-κB responsiveness to ouabain in cells expressing GFP-NKAα1.M32 with neighboring cells that only expressed the endogenous Na,K-ATPase α1-subunit. Fig. 6*a* shows a GFP-NKAα1.M32-expressing cell, and Fig. 6*b* shows NF-κB staining of this cell and its neighboring, untransfected cells in the same field of view following ouabain treatment for 30 min. NF-κB activation was semiquantitatively estimated by measuring the ratio of NF-κB nuclear signal to cytosolic signal for each cell in the same field of view. Results from this analysis indicated that ouabain caused nuclear translocation of NF-κB in non-transfected cells but was without effect in GFP-NKAα1.M32-expressing cells (Fig. 6*c*). These findings demonstrate that truncation of the NH_2 terminus of Na,K-ATPase α1-subunit results in a functional Na,K-ATPase that resides at the plasma membrane yet is sufficient to disrupt ouabain-induced activation of NF-κB.

DISCUSSION

It is now generally agreed that many, if not most, important processes in the cell are controlled by proteins aggregated together in complexes (21, 22, 31–33). The assembly of complexes that contain a receptor and components of signal machinery provides the cell with a highly selective means to engage a specific signaling pathway. The finding that ligand-bound Na,K-ATPase assembles with InsP$_3$R and that this assembly can give rise to intracellular Ca^{2+} oscillations with a constant periodicity in the minute range represents a novel principle for such a protein complex.

Based on our combined results, we suggest that the ouabain-induced Ca^{2+} oscillation and signal-transducing function of Na,K-ATPase is made possible by the local organization of Na,K-ATPase and InsP$_3$R into a spatially organized functional microdomain that links the plasma membrane to intracellular ER Ca^{2+} stores. A signaling microdomain can function without a diffusible messenger provided that the transducer and the effector are in such proximity that they can communicate via protein-protein interaction, either directly or via one or more interacting/scaffolding proteins. Molecular strategies using the InsP$_3$ sponge and pharmacological studies using the PLC inhibitor, U73122, indicate that the ouabain-induced Ca^{2+} oscillatory response may be elicited via an InsP$_3$-independent mechanism of InsP$_3$R activation. Significant energy transfer between the donor and acceptor complexes, GFP-NKAα1 and anti-InsP$_3$R-anti-mouse IgG-Cy3, indicate a distance of less than 12 nm (16). It is well established that the ER is juxtaposed to the plasma membrane (34). FRET was recorded in a region of the plasma membrane, and the result is clearly compatible with previous electron microscopy studies showing that the distance between the plasma membrane, where Na,K-ATPase is located, and the membrane of ER, where the InsP$_3$R is located, can be as short as 10 nm (35). It should be noted, however, that FRET is recorded between the GFP-labeled Na,K-ATPase and Cy3-labeled goat-anti-mouse IgG antibody that binds to the InsP$_3$R antibody. Taking the size of the antibodies and the GFP molecule into account, the maximal

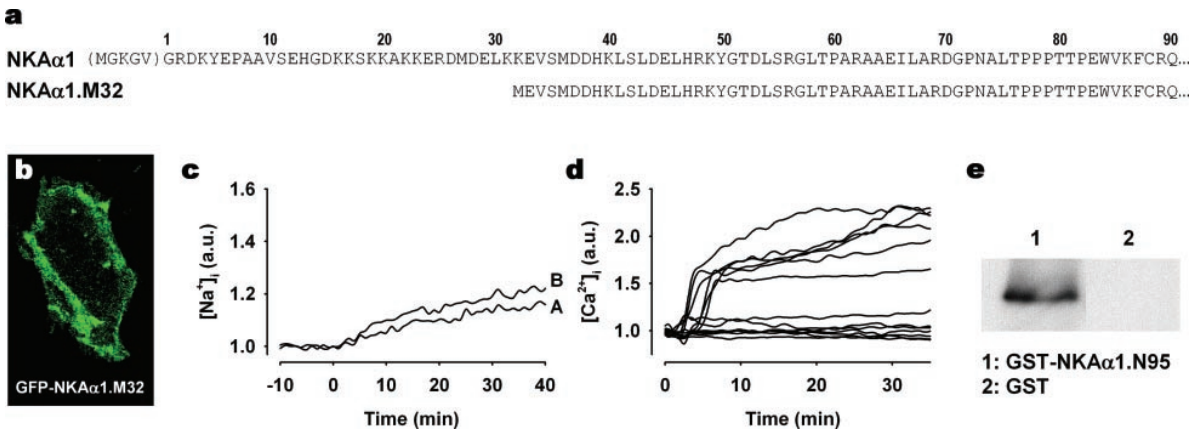

FIG. 5. **Role of NH_2 terminus of Na,K-ATPase α1-subunit in ouabain-induced Ca^{2+} signaling.** *a*, NH_2 terminus of the rat Na,K-ATPase α1-subunit and deletion mutant thereof. Numbering is based on the mature rat α1-subunit amino acid sequence (47). *b*, confocal microscope image of a GFP-NKAα1.M32-expressing RPT cell, recorded with a small pinhole to optimize membrane signal. *c*, intracellular Na^+ measurements following ouabain treatment (at time 0) in RPT cells expressing GFP-NKAα1.M32 (*trace A*) and endogenous Na,K-ATPase α1-subunit (*trace B*). Arbitrary units (*a.u.*) represent ratio values corresponding to intracellular Ca^{2+} and Na^+ concentration changes. *d*, single cell recordings of intracellular Ca^{2+} response to ouabain in GFP-NKAα1.M32-expressing RPT cells. No Ca^{2+} oscillations were observed. *e*, GST pull-down assay with RPT cell lysate followed by Western blotting for $InsP_3R3$.

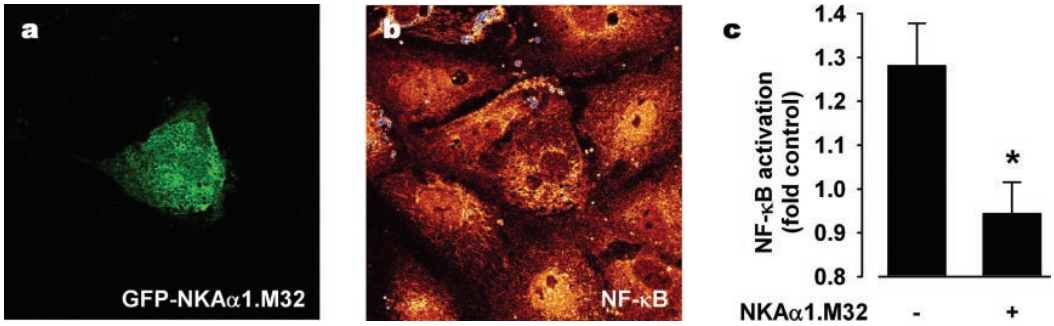

FIG. 6. **NF-κB translocation in GFP-NKAα1.M32-expressing cells following ouabain treatment.** *a*, GFP-NKAα1.M32-expressing RPT cell identified by GFP fluorescence. Images were recorded with an open pinhole to measure semiquantitatively the ratio between NF-κB abundance in the nucleus and cytosol. *b*, NF-κB immunosignal of GFP-NKAα1.M32-expressing and non-expressing RPT cells, from the same field of view as *a*. *c*, NF-κB activation in GFP-NKAα1.M32-expressing ($n = 47$) and non-expressing ($n = 218$) cells following ouabain treatment, mean ± S.E., *, $p < 0.05$. Ouabain-induced NF-κB nuclear translocation was abrogated in GFP-NKAα1.M32-expressing cells.

distance between Na,K-ATPase and $InsP_3R$ could be somewhat larger than the working distance for FRET fluorophores, GFP and Cy3. Hence, the FRET results do not rule out the possibility that Na,K-ATPase and $InsP_3R$ may interact via a scaffolding protein. The observed increase in FRET between Na,K-ATPase and $InsP_3R$ following ouabain exposure and the loss of FRET upon CytD treatment indicate that ouabain-induced Ca^{2+} oscillations were dependent on a dynamic physical association between Na,K-ATPase and $InsP_3R$ and therefore add further evidence to the concept that the Ca^{2+} signal arises from a signaling microdomain containing Na,K-ATPase and $InsP_3R$.

The question remains as to how the localization of Na,K-ATPase and $InsP_3R$ is controlled. As evidenced by our FRET and co-immunoprecipitation studies using CytD, an intact cytoskeleton is required for the physical association between Na,K-ATPase and $InsP_3R$ and ouabain-induced Ca^{2+} signaling. This suggests that actin, or cytoskeletal proteins associated with actin, will stabilize the Na,K-ATPase/$InsP_3R$ complex by physical tether cross-linking. Ankyrins, a family of adaptor proteins believed to participate in the organization of proteins into specialized regions in the plasma membrane and ER Ca^{2+} stores, represent an interesting putative mechanistic partner for orchestrating Na,K-ATPase and $InsP_3R$ proximity (25). The complete framework of adaptor and scaffolding proteins that may be involved in facilitating the structure and signal-transducing function of this microdomain is still uncertain, but our results also do not preclude the necessity of a direct physical interaction between Na,K-ATPase and $InsP_3R$ in this event. The activation of $InsP_3R$ is likely due to an allosteric effect of ouabain on Na,K-ATPase. Na,K-ATPase is a P-type ATPase that can exist in distinct E_1 and E_2 conformational states that are at least partially determined by intramolecular interactions between the NH_2 terminus and cytoplasmic loops of the enzyme. Ouabain binds to the E_2 conformation of the Na,K-ATPase and causes a robust shift in the E_1/E_2 poise toward E_2 forms (36). Information derived from the crystal structure of another P-type ATPase, the SERCA pump, suggests that the $E_1 \rightarrow E_2$ state transition is accompanied by significant movement of the three cytoplasmic domains, N (nucleotide binding), P (phosphorylation), and A (actuator) (37). A recent study (28) suggests that the NH_2 terminus may act as an auto-regulatory domain, modulating E_1/E_2 conformational transition. In E_1 conformation, the NH_2 terminus is in association with the first cytoplasmic loop of Na,K-ATPase. Transition from E_1 to E_2 conformation may release the NH_2 terminus from its interaction with the first cytoplasmic loop of Na,K-ATPase, thus making the NH_2 terminus available for interaction either with the $InsP_3R$ directly or with a protein bridging between Na,K-ATPase and $InsP_3R$. Such an effect could explain why truncation of the first 32 amino acids of the NH_2 terminus will prevent ouabain-induced Ca^{2+} oscillations. An alternative explanation is that NH_2-terminal truncation has

displaced the $E_1 \rightarrow E_2$ conformation of Na,K-ATPase in favor of E_1 (8, 38).

The concept that Na,K-ATPase may, in addition to its function as an ion pump, also act as a signal transducer, is now rapidly evolving (2–5). Most previous studies on the signaling role of Na,K-ATPase have been carried out on cardiac myocytes (for a review, see Ref. 39). In these cells, activation of Src kinase was found to be the primary event in the signaling cascade initiated by the ouabain/Na,K-ATPase complex, and downstream effects included phosphorylation of epidermal growth factor receptor and activation of the mitogen-activated protein kinase pathway. Since cardiac myocytes exhibit spontaneous Ca^{2+} sparks of high frequency, it has not yet been possible to establish whether Na,K-ATPase/InsP$_3$R-triggered Ca^{2+} oscillations also occur in these cells. Another model where Na,K-ATPase-mediated Ca^{2+} signaling is dependent on a close proximity between the plasma membrane and ER Ca^{2+} stores has been presented previously (40). In this model, Na,K-ATPase α2- and α3-subunits modulate Ca^{2+} release from ER via local changes in intracellular Na^+ concentration. Our study was performed on cells expressing only the α1-subunit of Na,K-ATPase, and the results from the protocols with the truncated NKAα1.M32 imply that increased intracellular Na^+ concentration was, in our model, not the main cause of ouabain-induced Ca^{2+} oscillations. Furthermore, we previously established that increasing intracellular Na^+, by lowering extracellular K^+ to the same extent as 250 μM ouabain, is not sufficient to elicit a Ca^{2+} oscillatory response (2).

Ca^{2+} oscillations trigger such universal processes as fertilization, cell division, cell differentiation, and apoptosis (41). The specificity of this signal is encoded by the frequency and/or the amplitude of the Ca^{2+} oscillations (42). In the case of G-protein-coupled receptors, Ca^{2+} oscillations generally have a periodicity of seconds (30, 43). The highly regular ouabain/Na,K-ATPase-induced Ca^{2+} oscillations displayed a longer periodicity in the minute range and should thereby provide a mechanism to ensure a different kind of physiological readout.

Endogenous ouabain levels are high during pregnancy and in the perinatal period (44, 45). Thus, it is of great physiological interest that the ouabain-induced slow Ca^{2+} oscillations were found to activate NF-κB. This pluripotent transcription factor activates genes modulating cell proliferation, apoptosis, and development as well as responses of the immune system (46). Cells expressing GFP-NKAα1.M32 did not respond to ouabain with Ca^{2+} oscillations. In these cells, ouabain did not activate NF-κB. These findings support the physiological significance of a signaling microdomain containing Na,K-ATPase α1-subunit and InsP$_3$R as a trigger mechanism for NF-κB activation.

In conclusion, we have demonstrated the existence of a cell signaling microdomain containing Na,K-ATPase and InsP$_3$R that acts as a signaling pathway for Ca^{2+} oscillations and activation of NF-κB. Our findings represent, in many aspects, a novel mechanism for generation of Ca^{2+} signaling where an ion pump, Na,K-ATPase, also functions as a signal transducer. The physiological importance of slow Ca^{2+} oscillations is generally recognized, yet few biological generators of this signal have been identified previously.

Acknowledgments—We thank Dr. Christian Broberger for fruitful discussions and Eivor Zettergren Markus for experimental assistance.

REFERENCES

1. Skou, J. C., and Esmann, M. (1992) *J. Bioenerg. Biomembr.* **24,** 249–261
2. Aizman, O., Uhlen, P., Lal, M., Brismar, H., and Aperia, A. (2001) *Proc. Natl. Acad. Sci. U. S. A.* **98,** 13420–13424
3. Haas, M., Askari, A., and Xie, Z. (2000) *J. Biol. Chem.* **275,** 27832–27837
4. Lichtstein, D., McGowan, M. H., Russell, P., and Carper, D. A. (2000) *Hypertens. Res.* **23,** (suppl.) S51–S53
5. Peng, M., Huang, L., Xie, Z., Huang, W. H., and Askari, A. (1996) *J. Biol. Chem.* **271,** 10372–10378
6. Haux, J. (1999) *Med. Hypotheses* **53,** 543–548
7. Repke, K. R., Schon, R., Megges, R., Weiland, J., Nissen, E., and Matthes, E. (1995) *Anti-Cancer Drug Des.* **10,** 177–187
8. Daly, S. E., Lane, L. K., and Blostein, R. (1996) *J. Biol. Chem.* **271,** 23683–23689
9. Zelenina, M., Zelenin, S., Bondar, A. A., Brismar, H., and Aperia, A. (2002) *Am. J. Physiol.* **283,** F309–F318
10. Uchiyama, T., Yoshikawa, F., Hishida, A., Furuichi, T., and Mikoshiba, K. (2002) *J. Biol. Chem.* **277,** 8106–8113
11. Uhlen, P., Laestadius, A., Jahnukainen, T., Soderblom, T., Backhed, F., Celsi, G., Brismar, H., Normark, S., Aperia, A., and Richter-Dahlfors, A. (2000) *Nature* **405,** 694–697
12. Belusa, R., Wang, Z. M., Matsubara, T., Sahlgren, B., Dulubova, I., Nairn, A. C., Ruoslahti, E., Greengard, P., and Aperia, A. (1997) *J. Biol. Chem.* **272,** 20179–20184
13. Sugiyama, T., Furuya, A., Monkawa, T., Yamamoto-Hino, M., Satoh, S., Ohmori, K., Miyawaki, A., Hanai, N., Mikoshiba, K., and Hasegawa, M. (1994) *FEBS Lett.* **354,** 149–154
14. Kenworthy, A. K. (2001) *Methods* (*Orlando*) **24,** 289–296
15. Wouters, F. S., Verveer, P. J., and Bastiaens, P. I. (2001) *Trends Cell Biol.* **11,** 203–211
16. Ng, T., Squire, A., Hansra, G., Bornancin, F., Prevostel, C., Hanby, A., Harris, W., Barnes, D., Schmidt, S., Mellor, H., Bastiaens, P. I., and Parker, P. J. (1999) *Science* **283,** 2085–2089
17. Hamlyn, J. M., Blaustein, M. P., Bova, S., DuCharme, D. W., Harris, D. W., Mandel, F., Mathews, W. R., and Ludens, J. H. (1991) *Proc. Natl. Acad. Sci. U. S. A.* **88,** 6259–6263
18. Bootman, M. D., Collins, T. J., Mackenzie, L., Roderick, H. L., Berridge, M. J., and Peppiatt, C. M. (2002) *FASEB J.* **16,** 1145–1150
19. Peppiatt, C. M., Collins, T. J., Mackenzie, L., Conway, S. J., Holmes, A. B., Bootman, M. D., Berridge, M. J., Seo, J. T., and Roderick, H. L. (2003) *Cell Calcium* **34,** 97–108
20. Tang, T. S., Tu, H., Chan, E. Y., Maximov, A., Wang, Z., Wellington, C. L., Hayden, M. R., and Bezprozvanny, I. (2003) *Neuron* **39,** 227–239
21. Yang, J., McBride, S., Mak, D. O., Vardi, N., Palczewski, K., Haeseleer, F., and Foskett, J. K. (2002) *Proc. Natl. Acad. Sci. U. S. A.* **99,** 7711–7716
22. Johenning, F. W., and Ehrlich, B. E. (2002) *Neuron* **34,** 173–175
23. Felder, C. C. (1995) *FASEB J.* **9,** 619–625
24. Monkawa, T., Miyawaki, A., Sugiyama, T., Yoneshima, H., Yamamoto-Hino, M., Furuichi, T., Saruta, T., Hasegawa, M., and Mikoshiba, K. (1995) *J. Biol. Chem.* **270,** 14700–14704
25. Bourguignon, L. Y., Jin, H., Iida, N., Brandt, N. R., and Zhang, S. H. (1993) *J. Biol. Chem.* **268,** 7290–7297
26. Devarajan, P., Scaramuzzino, D. A., and Morrow, J. S. (1994) *Proc. Natl. Acad. Sci. U. S. A.* **91,** 2965–2969
27. Jorgensen, P. L., Skriver, E., Hebert, H., and Maunsbach, A. B. (1982) *Ann. N. Y. Acad. Sci.* **402,** 207–225
28. Segall, L., Lane, L. K., and Blostein, R. (2002) *J. Biol. Chem.* **277,** 35202–35209
29. Daly, S. E., Lane, L. K., and Blostein, R. (1994) *J. Biol. Chem.* **269,** 23944–23948
30. Dolmetsch, R. E., Xu, K., and Lewis, R. S. (1998) *Nature* **392,** 933–936
31. Delmas, P., Wanaverbecq, N., Abogadie, F. C., Mistry, M., and Brown, D. A. (2002) *Neuron* **34,** 209–220
32. Simons, K., and Toomre, D. (2000) *Nat. Rev. Mol. Cell. Biol.* **1,** 31–39
33. Kiselyov, K., Xu, X., Mozhayeva, G., Kuo, T., Pessah, I., Mignery, G., Zhu, X., Birnbaumer, L., and Muallem, S. (1998) *Nature* **396,** 478–482
34. Berridge, M. J. (1998) *Neuron* **21,** 13–26
35. Ichitani, Y., Holmberg, K., Maunsbach, A. B., Haeggstrom, J. Z., Samuelsson, B., De Witt, D., and Hokfelt, T. (2001) *Cell Tissue Res.* **303,** 235–252
36. Lingrel, J. B., Arguello, J. M., Van Huysse, J., and Kuntzweiler, T. A. (1997) *Ann. N. Y. Acad. Sci.* **834,** 194–206
37. Toyoshima, C., Nakasako, M., Nomura, H., and Ogawa, H. (2000) *Nature* **405,** 647–655
38. Boxenbaum, N., Daly, S. E., Javaid, Z. Z., Lane, L. K., and Blostein, R. (1998) *J. Biol. Chem.* **273,** 23086–23092
39. Xie, Z., and Askari, A. (2002) *Eur. J. Biochem.* **269,** 2434–2439
40. Blaustein, M. P., and Golovina, V. A. (2001) *Trends Neurosci.* **24,** 602–608
41. Berridge, M. J., Bootman, M. D., and Roderick, H. L. (2003) *Nat. Rev. Mol. Cell. Biol.* **4,** 517–529
42. Berridge, M. J., Lipp, P., and Bootman, M. D. (2000) *Nat. Rev. Mol. Cell. Biol.* **1,** 11–21
43. De Koninck, P., and Schulman, H. (1998) *Science* **279,** 227–230
44. Di Bartolo, V., Balzan, S., Pieraccini, L., Ghione, S., Pegoraro, S., Biver, P., Revoltella, R., and Montali, U. (1995) *Life Sci.* **57,** 1417–1425
45. Vakkuri, O., Arnason, S. S., Pouta, A., Vuolteenaho, O., and Leppaluoto, J. (2000) *J. Endocrinol.* **165,** 669–677
46. Rothwarf, D. M., and Karin, M. (1999) *Science's STKE* http://stke.sciencemag.org/cgi/content/full/OCsigtrans;1999/5/re1
47. Shull, G. E., Greeb, J., and Lingrel, J. B. (1986) *Biochemistry* **25,** 8125–8132